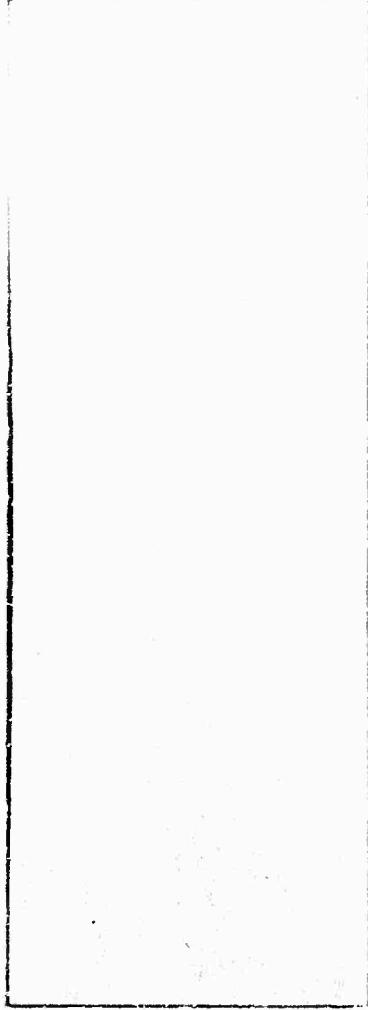


AD626816



PHILCO.

A SUBSIDIARY OF *Ford Motor Company.*

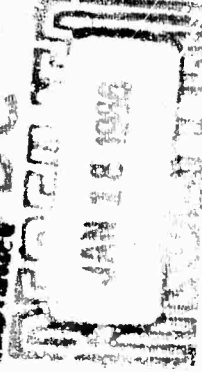
AERONAUTRONIC DIVISION

PROPERTY

OF

GOSSARD SPACE FLIGHT CENTER

LIBRARY DC



YISA 3

28698

DISCLAIMER NOTICE

THIS DOCUMENT IS THE BEST
QUALITY AVAILABLE.
COPY FURNISHED CONTAINED
A SIGNIFICANT NUMBER OF
PAGES WHICH DO NOT
REPRODUCE LEGIBLY.

Under Contract: NOnr 3560(00)
ARPA Order No. 273/11-7-63


6 August 1965

SCIENTIFIC REPORT

ABSORPTION BY CO₂ BETWEEN 8000 AND 10,000 cm⁻¹
(1 - 1.25 Micron Region)

Prepared for: Advanced Research Projects Agency
Washington 25, D. C.

Prepared by: Darrell E. Burch
David A. Gryvnak
Richard R. Patty

Approved: 
M. H. Johnson, Director
Physics Laboratory

"This material is the result of tax-supported research and as such may be freely reprinted with the customary crediting of the source."


AERONUTRONIC
DIVISION OF PHILCO CORPORATION
A SUBSIDIARY OF *Ford Motor Company*
FORD ROAD, NEWPORT BEACH, CALIF.

ABSTRACT

The absorption by CO_2 in the 9300 to 9650 cm^{-1} region (1.0 μ) and 8000 to 8325 cm^{-1} region (1.2 μ) have been studied. Spectra were obtained for four samples of CO_2 in the 1.0 μ region at a pressure of 2.5 atmospheres and path lengths up to 933 meters. Spectra were obtained for ten samples of CO_2 in the 1.2 μ region at pressures as high as 15 atmospheres for path lengths up to 32.9 meters and pressures as high as 2.50 atmospheres for path lengths up to 933 meters. The strengths of the important bands and the half-widths of several lines have been measured. Tables of transmittance versus wavenumber are included for both regions as well as photographs of most of the spectra. Also presented are tables of the integrated absorbance $\int_{\nu}^{\nu'} A(\nu) d\nu$ versus ν for both regions.

TABLE OF CONTENTS

SECTION		PAGE
1	INTRODUCTION AND SUMMARY.	1-1
2	EXPERIMENTAL METHODS AND NOTATION	2-1
	2.1 Apparatus and Procedure.	2-1
	2.2 Definitions, Symbols and Notations	2-2
3	DISCUSSION OF ABSORPTION BANDS.	3-1
	3.1 Identification and Features of the Absorption Bands	3-1
	Table 3-1, Positions and Strenghths of	
	Absorption Bands.	3-2
	Figure 3-1, Transmission Spectra of the	
	9300-9650 cm^{-1} Region	3-4
	Figure 3-2, Transmission Spectra of the	
	8000-8350 cm^{-1} Region	3-5
	Figure 3-3, Transmission Spectra of the	
	8000-8350 cm^{-1} Region	3-6
	Table 3-2, Sample Parameters	3-7
	3.2 Band Strengths	3-8
	3.3 Half-Widths of Absorption Lines.	3-11
	Figure 3-4, Half-Widths of Self-Broadened	
	CO ₂ Lines at 1 Atm. Pressure	3-13
4	TABLES OF TRANSMITTANCE	4-1
	Table 4-1, Table of Transmittances (9340-9660 cm^{-1}) . .	4-2
	Table 4-2, Table of Transmittances (8030-8340 cm^{-1}) . .	4-3
5	TABLES OF INTEGRATED ABSORPTANCE.	5-1
	Table 5-1, Table of Integrated Absorptance	
	(9430-9660 cm^{-1})	5-2
	Table 5-2, Table of Integrated Absorptance	
	(8030-8340 cm^{-1})	5-3
6	REFERENCES.	6-1

(This page is intentionally left blank.)

SECTION 1

INTRODUCTION AND SUMMARY

Most of the important absorption bands of CO_2 in the region between 8000 and 10,000 cm^{-1} have been observed by Herzberg and Herzberg.¹ These workers contained their samples in a multiple-pass absorption cell which was capable of very long paths and obtained their spectra photographically. They measured the positions of many of the lines and the centers of several of the bands with very good accuracy; but very little can be learned about the strengths or widths of the absorption lines from their data.

The present investigation was undertaken to obtain spectra of samples covering a wide range of pressures and path lengths. From the results included in this report, the strengths of nearly all of the lines of any importance and the widths of several of them can be determined. From this information, one can, at least in principle, calculate the transmission over an extremely wide variation of paths, including those in which the pressure, temperature and the mixing ratio of CO_2 with other gases might vary.

The band near 9500 cm^{-1} is of particular importance at the present time in the interpretation of spectra of the atmospheres of Mars and Venus. It occurs in a region free of absorption lines of other atmospheric gases; therefore, spectra of the planetary atmospheres can be obtained from the earth's surface. This band is so weak that its integrated absorptance in the Martian atmosphere should be very nearly independent of the pressure of the gas. Thus, by comparing the planetary spectra with laboratory spectra such as some of those presented below, one should be able to determine the amount of CO_2 in the Martian atmosphere.

Once the amount of CO_2 is known, the pressure can be determined by investigating other bands in which the absorption is a function of both the amount of CO_2 and the total pressure.

Spectra of several samples are shown in Section 3 with a discussion of the various features of the bands. The strengths, or absolute intensities, of the important bands have been determined, and the half-widths of several of the lines have been measured. Section 4 includes a table of transmittance versus wavenumber for 14 different samples studied. Section 5 contains tables of the integrated absorbance $\int A(\nu) d\nu$ for the same samples; from this table the integrated absorbance over virtually any region of interest in the bands can be determined.

SECTION 2

EXPERIMENTAL METHODS AND NOTATION

2.1 APPARATUS AND PROCEDURE

Samples of CO_2 were contained in two different absorption cells which have been described previously.² The longer cell has a base length of approximately 30 meters and was used at as many as 32 passes, giving a total path length of 933 meters. It is approximately 0.9 meters in diameter and can be evacuated to less than one micron of Hg or pressurized to as much as 2.5 atmospheres. The shorter cell has a base length of approximately 1 meter and was used at as many as 32 passes. It can be evacuated or pressurized to as much as 15 atmospheres.

The CO_2 was drawn from the vapor in a dewar which contained both liquid and vapor at a pressure of about 300 psig and a temperature of approximately -20°C . We found that samples obtained in this manner contained fewer impurities, particularly H_2O , than samples taken from commercial cylinders at room temperature. A spectrum published previously by us shows a small amount of absorption in the region between approximately 9530 and 9560 cm^{-1} which is apparently due to an impurity since the absorption does not appear in more recent spectra of samples obtained in the manner described above.

The spectra were obtained with an Ebert type spectrometer whose main mirror has a 75 cm focal length. The region from 9000 to $10,000\text{ cm}^{-1}$ was scanned with a grating having 1200 lines/mm and blazed at $0.8\text{ }\mu$. It was used in the first order and a Tiffen glass filter eliminated overlapping orders of shorter wavelengths. The region between 8000 and 9000 cm^{-1} was studied with a grating having 300 lines/mm and blazed at $3.2\text{ }\mu$. Overlapping orders were eliminated in this region by the use of a silicon window. Both gratings have a ruled area of $64 \times 64\text{ mm}$.

A PbS cell cooled with liquid nitrogen was used as the detector. It was not necessary to cool the detector below dry ice temperature for operation in this wavelength region, but the dewar on the detector was designed to hold liquid nitrogen for use at longer wavelengths. Cooling by liquid nitrogen was, therefore, more convenient and was used since the signal-to-noise ratio was approximately the same at both temperatures. A considerably better signal-to-noise ratio (S/N) could probably be achieved in the region between 9000 and 10,000 cm^{-1} with a photomultiplier detector. However, the extra sensitivity of the photomultiplier was not required in order to obtain spectra from which the strengths of the bands in this region can be determined. The S/N in the 8000 - 9000 cm^{-1} region was enough higher than in the higher wavenumber region that we could conveniently work with a smaller spectral slitwidth. Most of the spectra in the lower wavenumber region were obtained with sufficiently good spectral resolution that many of the lines could be resolved. However, in the higher wavenumber region the slits were opened until a desirable S/N was obtained.

Wavenumber calibration was obtained for each spectrum from the positions of the absorption lines and band centers designated in Figures 3-1 and 3-2, most of which are from Herzberg and Herzberg.¹

The raw spectra were replotted and digitized by the use of apparatus described in Appendix C of reference 2. A computer program was then used to calculate values of transmittance and integrated absorbance which are shown in Sections 4 and 5.

2.2 DEFINITIONS, SYMBOLS AND NOTATIONS

L is the geometrical path length of the radiation as it passes through a sample, p is the pressure of the CO_2 which is measured in atmospheres unless otherwise specified, and u is the absorber thickness given by

$$u = W p L \frac{273}{296} \text{ (atm cm}_{\text{STP}}\text{)}. \quad (2-1)$$

W is a factor that accounts for the Van der Waals' forces which cause CO_2 to deviate from a perfect gas at some of the pressures used in this investigation. It is given adequately for our purposes by

$$W = 1.00 + 0.0047 p. \quad (2-2)$$

The quantity $273/296$ accounts for the difference in density between standard temperature (273°K) and room temperature (296°K) at which all of the measurements were made. The absorber thickness given by Equation (2-1) is then equivalent to the thickness of a CO_2 sample at 1 atmosphere pressure and 273°K having the same number of molecules per unit area as the sample being described.

Although this investigation deals only with samples of pure CO₂, it is frequently desirable to relate the pressures to an equivalent pressure P_e of a dilute mixture of CO₂ in N₂. This is necessary when dealing with paths through the earth's atmosphere in which the partial pressure of CO₂ is small compared to that of N₂. Burch, Gryvnak and Williams⁴ have found that throughout most of the spectrum an equivalent pressure given by

$$P_e = 1.3 p + (P - p) \quad (2-3)$$

can be used where P is the total pressure due to both gases. It is noted that the equivalent pressure approaches the total pressure for a very dilute mixture of CO₂ in N₂. The factor 1.3 relates the self-broadening ability of CO₂ to the broadening ability of CO₂ lines by N₂. It is valid in regions where most of the absorption is due to lines whose centers are within a few cm⁻¹; but it is not valid in regions such as on the high wavenumber side of the ν₃ and 3ν₃ bands where the absorption is due to the extreme wings of lines whose centers are several cm⁻¹ away. Variations in the shapes of the extreme wings of CO₂ absorption lines give rise to the difference in the relative broadening abilities. The line shapes of different broadening gases will be discussed in a report⁵ to be published by us in the near future.

Since the simple classical theory predicts that the half-width of a line is proportional to the density of molecules, Equation (2-3) should probably be modified to account for the non-linearity between pressure and density at higher pressures. The modification can be made in the following way:

$$P_e = 1.3 W p + (P - p). \quad (2-3')$$

T(ν) is the observed transmittance and A(ν) ≡ 1 - T(ν) is the observed absorbance. T'(ν) and A'(ν) are the transmittance and absorbance, respectively, which would be observed with an instrument having infinite resolving power. T'(ν) is related to the absorption coefficient K(ν) by

$$T'(\nu) = \exp \left[-u K(\nu) \right] \quad \text{or} \quad -\ln T'(\nu) = u K(\nu). \quad (2-4)$$

α is the half-width of an absorption line and is expressed in cm⁻¹. S_ν is the band strength, or band intensity, and is related to the absorption coefficient due to the band of interest by

$$S_\nu = \int K(\nu) d\nu. \quad (2-5)$$

(This page is intentionally left blank.)

SECTION 3

DISCUSSION OF ABSORPTION BANDS

3.1 IDENTIFICATION AND FEATURES OF THE ABSORPTION BANDS

All of the CO_2 bands which one might expect to produce appreciable absorption in the region from 8000 to $10,000\text{ cm}^{-1}$ are listed in Table 3-1. The positions of the band centers measured by Herzberg and Herzberg¹ and by Courtois⁶ are listed. Centers of the other bands were calculated from energy levels tabulated by Stull, Wyatt and Plass.⁷ In the notation for the transitions, the lower level is omitted when it is 00^00 . The strengths of the different portions of the bands are described in Section 3.2.

The bands occur in two groups, one between 9300 and 9650 cm^{-1} and the other between 8000 and 8325 cm^{-1} . All of the bands arise from transitions in which there is a change of three (3) in ν_3 , the quantum number associated with ν_3 . Since, for CO_2 , $\nu_1 = 2\nu_2$, the bands arising from transitions from the ground state to 20^03 , 1^003 , and 04^00 occur close to each other. These bands, along with their associated difference bands, occur in the region from 9300 to 9650 cm^{-1} . The changes in each of the quantum numbers are the same for the difference bands as for the combination bands, but the difference bands arise from transitions from the 01^10 state.

Because of anharmonicity, a difference band usually occurs at a slightly lower wavenumber than its associated combination or fundamental band. However, the displacement of the difference band varies from one band to another, depending on the Fermi resonance.

TABLE 3-1
POSITIONS AND STRENGTHS OF ABSORPTION BANDS

Band Center cm ⁻¹	Transition ^a	Portion	Strength cm ⁻¹ atm ⁻¹ STP	Strength cm ⁻¹ x 10 ⁻⁵
9631.38 HH ^b	20 ⁰ 3	R-Branch P-Branch Entire Band	1.4 1.25 2.6	+ 0.13 x 10 ⁻⁵ + 0.14 x 10 ⁻⁵ - 0.25 x 10 ⁻⁵
9629.6 SWP	21 ¹ 3-01 ¹ 0	Entire Band ^c	2.0	x 10 ⁻⁶
9517.00 HH	12 ⁰ 3	R-Branch P-Branch Entire Band	3.40 3.23 6.63	+ 0.2 x 10 ⁻⁵ + 0.5 x 10 ⁻⁵ - 0.7 x 10 ⁻⁵
9478.2 SWP	13 ¹ 3-01 ¹ 0	Entire Band ^c	5.2	x 10 ⁻⁶
9389.02 HH	04 ⁰ 3	R-Branch P-Branch Entire Band	6.5 5.5 12.5	+ 0.7 x 10 ⁻⁶ + 1 x 10 ⁻⁶ - 1.5 x 10 ⁻⁶
9320.1 SWP	05 ¹ 3-01 ¹ 0		Not measurable	
8294.01 HH	10 ⁰ 3	R-Branch P-Branch Entire Band	8.4 8.6 17.0	+ 0.6 x 10 ⁻⁴ + 0.6 x 10 ⁻⁴ - 1.0 x 10 ⁻⁴
8276.83 HH	11 ¹ 3-01 ¹ 0	Entire Band ^c	1.5	x 10 ⁻⁴
8243.2 SWP	20 ⁰ 3-10 ⁰ 0		Not observable	
8231.6 SWP	12 ⁰ 3-02 ⁰ 0		Not observable	
8220.0 SWP	10 ⁰ 3 (C ¹² O ¹⁶ O ¹⁸)		Not observable	
8192.62 HH	02 ⁰ 3	R-Branch P-Branch Entire Band	6.0 5.8 11.8	+ 0.5 x 10 ⁻⁴ + 0.5 x 10 ⁻⁴ - 0.9 x 10 ⁻⁴
8135.95 HH	(3 ¹ 3-01 ¹ 0	Entire Band	1.0	+ 0.2 x 10 ⁻⁴
8128.8 SWP	12 ⁰ 3-10 ⁰ 0		Not observable	
8119.7 SWP	02 ⁰ 3 (C ¹² O ¹⁶ O ¹⁸)		Not observable	
8103.7 SWP	04 ⁰ 3-02 ⁰ 0		Not observable	
8089.01 C	10 ⁰ 3 (C ¹³ O ¹⁶ ₂)	Entire Band	2.5	+ 1 x 10 ⁻⁵

^aTransitions for isotope C¹²O¹⁶₂ unless otherwise specified.

^bAuthority for position of band center. HH and C refer to Herzberg and Herzberg¹ and to Courtoy,⁶ respectively SWP denotes that band centers were calculated from energy levels tabulated by Stull, Wyatt and Plass.⁷

^cStrengths of difference bands were calculated from combined strengths of difference band and associated combination band by use of Equation (3-3).

Spectra of the $9390 - 9650 \text{ cm}^{-1}$ region are shown in Figure 3-1 with the positions of the band centers indicated in the lower panel. The curve in the lower panel is a replot of the original spectrum of the largest sample studied in this investigation; it was obtained with the spectral slitwidth sufficiently wide that the structure of the band was lost. The upper panel shows a photograph of an original spectrum of a different sample obtained with considerably narrower slits. This spectrum is rather noisy, but the structure in the P-branch of the three stronger bands is apparent. The magnitude of the noise in the spectrum can be seen in the region above about 9650 cm^{-1} , as well as in the regions just above the heads of the other bands. All the spectra used in the analysis were obtained with wider slits in order to reduce the noise to less than 2 or 3% of the signal.

The 20^0_3 and $21^1_3-01^1_0$ bands are not resolved and appear as a single band since their centers are separated by only about 1.8 cm^{-1} . The $13^1_3-01^1_0$ band overlaps the P-branch of the 12^0_3 band, with evidence of the head of the former at about 9495 cm^{-1} . The 04^0_3 band is weaker than the other two; its associated difference band ($05^1_3-01^1_0$ band) is very weak and is not included in the spectrum shown. Only a hint of absorption could be observed on the spectrum of our largest sample in the region where this band should occur.

The 10^0_3 and 02^0_3 bands are separated by approximately 100 cm^{-1} and occur in the region between 8000 and 8325 cm^{-1} along with their associated difference bands. Figures 3-2 and 3-3 show spectra of several different samples obtained in this region. The numbers enclosed in rectangles are the sample numbers listed in Table 3-2. The positions of the centers of the more important bands are indicated in the lower panel of Figure 3-2. The center of the $11^1_3-01^1_0$ band occurs in the P-branch of the 10^0_3 band with the head of the difference band near the center of the 10^0_3 band. The effect of the difference band on the absorption near 8280 cm^{-1} can be seen easily in the spectrum of Sample 8. The $03^1_3-01^1_0$ band also occurs in the P-branch of its associated combination band (02^0_3); its presence is more apparent since the band head occurs further from the center of the stronger band.

The difference bands due to transitions from the 02^0_0 and 10^0_0 states could probably be seen in the spectra of our largest samples if they were not overlapped by the lines of stronger bands. Resolution considerably better than that employed in this investigation would be required in order to observe the lines of these bands between the much stronger ones.

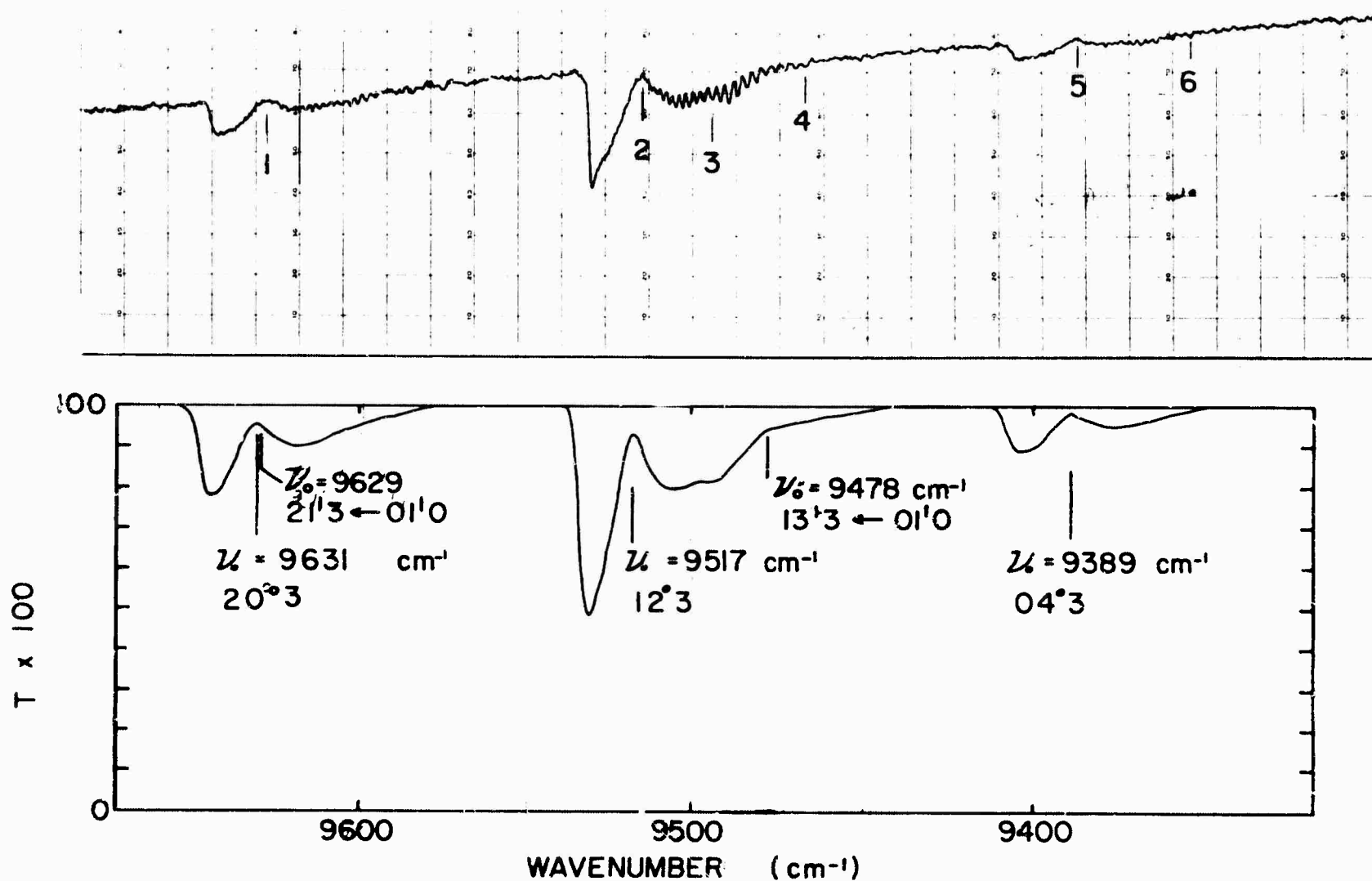
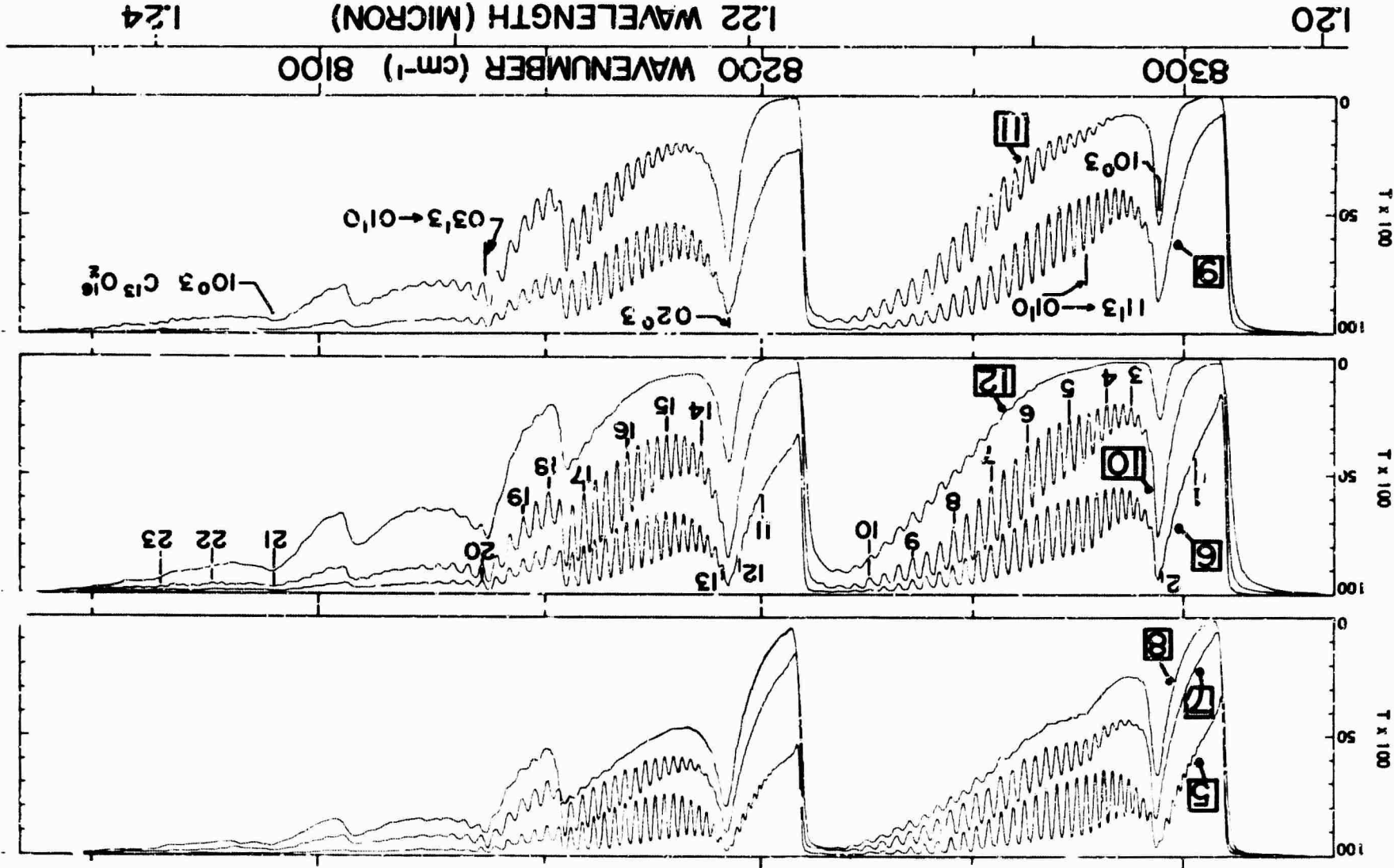


FIGURE 3-1 TRANSMISSION SPECTRA OF THE 9300 - 9650 cm^{-1} REGION.

The upper curve is a photograph of an original spectrum obtained with a slitwidth of about 1.3 cm^{-1} for a sample of pure CO_2 with $p = 2.50 \text{ atm}$ and $u = 10.9 \times 10^4 \text{ atm cm}_{\text{STP}}$. The lower curve was replotted from a spectrum of Sample 4 ($p = 2.50 \text{ atm}$, $u = 21.7 \times 10^4 \text{ atm cm}_{\text{STP}}$) with a spectral slitwidth of 3.8 cm^{-1} . The wavenumbers of the centers of the bands are indicated. Note that the wavenumber scales are not the same in both panels. Wavenumbers of the points indicated in the upper panel are: 1, 9631.4 cm^{-1} ; 2, 9517.00 cm^{-1} ; 3, 9495.33 cm^{-1} ; 4, 9467.50 cm^{-1} ; 5, 9389.02 cm^{-1} ; 6, 9356.23 cm^{-1} . These points were used for wavenumber calibration.

FIGURE 3-2 TRANSMISSION SPECTRA OF THE 8000 - 8350 cm^{-1} REGION.

The wavenumbers of the centers of the bands are indicated in the lower panel. Numbers enclosed in rectangles are sample numbers (See Table 3-2). Wavenumbers of the points indicated in the middle panel are: 1, 8302.4 cm^{-1} ; 2, 8294.8 cm^{-1} ; 3, 8287.2 cm^{-1} ; 4, 8281.4 cm^{-1} ; 5, 8272.5 cm^{-1} ; 6, 8262.4 cm^{-1} ; 7, 8254.1 cm^{-1} ; 8, 8245.1 cm^{-1} ; 9, 8235.5 cm^{-1} ; 10, 8225.2 cm^{-1} ; 11, 8200.0 cm^{-1} ; 12, 8194.8 cm^{-1} ; 13, 8191.0 cm^{-1} ; 14, 8185.9 cm^{-1} ; 15, 8178.0 cm^{-1} ; 16, 8169.1 cm^{-1} ; 17, 8159.0 cm^{-1} ; 18, 8150.7 cm^{-1} ; 19, 8144.9 cm^{-1} ; 20, 8135.6 cm^{-1} ; 21, 8089.6 cm^{-1} ; 22, 8076.4 cm^{-1} ; 23, 8065.2 cm^{-1} . These points were used for wavenumber calibration.

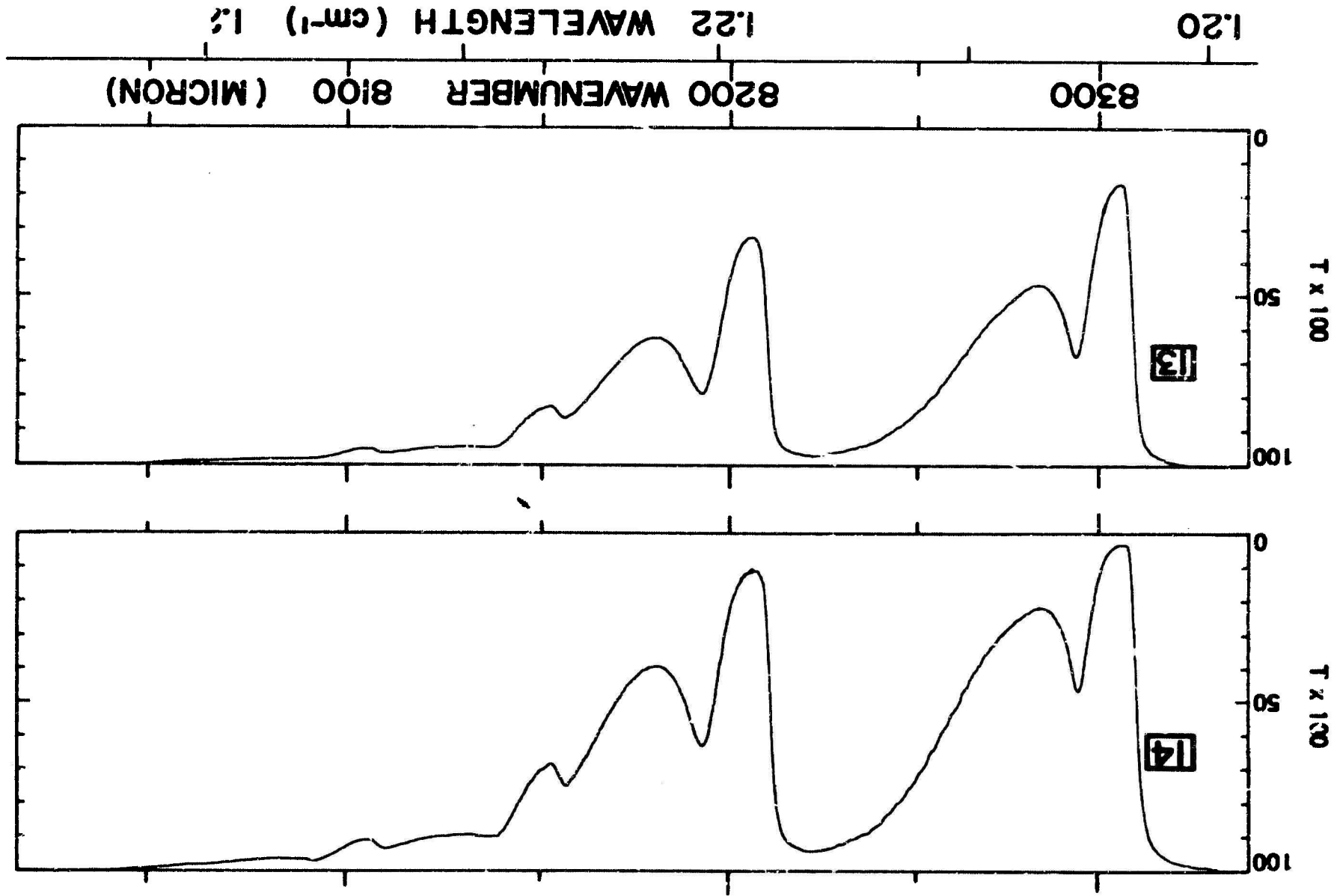


FIGURE 3-3 TRANSMISSION SPECTRA OF THE 8000 - 8350 cm^{-1} REGION.

The curves show spectra of samples 13 and 14 obtained at a pressure of 14.6 atm in order to smooth out the structure. These points were used for wavenumber calibration.

TABLE 3-2

SAMPLE PARAMETERS

Sample No.	P torr	P atm	u atm cm ² STP	L Path Meters	Spectral Slitwidth (cm ⁻¹)	Figure in which spectrum is shown
1	1900	2.50	5.51 x 10 ⁴	237	2.5	Not shown
2	1900	2.50	10.9 x 10 ⁴	469	2.5	Not shown
3	1900	2.50	16.3 x 10 ⁴	701	3.8	Not shown
4	1900	2.50	21.7 x 10 ⁴	933	3.8	3-1
5	758	0.997	1.11 x 10 ⁴	121	1.2	3-2
6	758	0.997	2.18 x 10 ⁴	237	1.5	3-2
7	758	0.997	4.32 x 10 ⁴	469	1.9	3-2
8	758	0.997	8.60 x 10 ⁴	933	2.8	3-2
9	1920	2.53	2.83 x 10 ⁴	121	1.5	3-2
10	1920	2.53	5.57 x 10 ⁴	237	1.5	3-2
11	1920	2.53	11.0 x 10 ⁴	469	1.9	3-2
12	1920	2.53	21.9 x 10 ⁴	933	2.8	3-2
13	11,100	14.6	2.38 x 10 ⁴	16.5	1.1	3-3
14	11,100	14.6	4.73 x 10 ⁴	32.9	1.1	3-3

The 10⁰3 band of C¹³O₂¹⁶ can be seen with its center at 8089.0 cm⁻¹. It was identified as 02⁰3 by Herzberg and Herzberg¹ and later identified as 10⁰3 by Courtoy.⁷ Stull, Wyatt and Plass⁷ give 8089.0 cm⁻¹ for the band center of 10⁰3 and 7981.1 cm⁻¹ for 02⁰3. The latter band is very weak and will be discussed in a future report covering the region between 7100 and 8000 cm⁻¹. The 10⁰3 and 02⁰3 bands of C¹²O₁₆¹⁸ should be sufficiently strong to be observed in the spectrum of our largest samples if they were not overlapped by lines of the stronger bands. Like the difference bands mentioned above, lines of these isotopic bands could probably be seen with better resolution. No attempt was made to change the relative abundances of the isotopes in our samples. It is probably safe to assume that they occur in their natural abundances.

It is noted that all of the bands in this region have a rather sharp band head on the high wavenumber side of the R-branch, a feature which is typical of CO₂ bands having a change in the quantum number ν_3 associated with ν_3 . The heads of the bands included in this report occur near $J = 44$ in the R-branch.

3.2 BAND STRENGTHS

The strength, or intensity, of an absorption band is given by

$$S_v = \int K(\nu) d\nu, \quad (2-5)$$

where the integration is performed over all ν for which there is appreciable absorption. $K(\nu)$, the absorption coefficient, is defined by Equation (2-4).

Of course, if more than one band contributes to the absorption at a given wavenumber, $K(\nu)$ used in Equation (2-5) must include only the portion due to the band whose strength is being determined. The methods used to estimate the contributions of each band in overlapping regions are described below.

The strengths of the bands included in this report are essentially independent of pressure over the range of pressures used. However, as the pressure is increased, the lines are broadened until at 14.6 atm, the maximum pressure used, the half-widths are of the order of 1.3 cm^{-1} . This is less than the spectral slitwidth used in obtaining spectra of Samples 13 and 14 (Figure 3-3). Consequently, the observed transmittance $T(\nu)$ is very nearly the true transmittance $T'(\nu)$. By combining Equations (2-4) and (2-5), we see that we can determine the band strengths from the spectra by use of the following equation.

$$S_v = -\frac{1}{u} \int \ln T(\nu) d\nu. \quad (3-1)$$

Equation (3-1) was used to determine the strengths of all the bands in the 8000 - 8325 cm^{-1} region from Samples 13 and 14, except for the 1003 band of Cl_2O . It was not possible to use samples in the shorter absorption cell with sufficiently large absorber thickness to produce more than a few percent absorbance by this band or by the bands in the 9300 - 9650 cm^{-1} region. Therefore, the strengths of these bands were determined from spectra of samples contained in the longer absorption cell whose maximum pressure is 2.5 atmospheres. At this pressure $T'(\nu)$ may be quite different from $T(\nu)$; but Equation (3-1) can still be used, provided $A(\nu) \approx 1 - T(\nu)$ is not too large. A more detailed discussion of the limitations on (3-1) when dealing with samples at relatively low pressures is given in Reference 8.

For Σ - Σ bands (quantum number $\mathcal{L} = 0$) of CO_2 , the strength S_m of a given line within a band is related to the band strength S_v by

$$S_m = S_v \left| m \right| \exp \left[-\frac{B'' m(m-1)}{k\theta} \right] / Q_r. \quad (3-2)$$

$m = J + 1$ for the R-branch and $-J$ for the P-branch. B'' is the rotational constant of the lower state, k is Boltzmann's constant, θ is the temperature, and Q_r is the rotational partition function. The Q-branch is missing in $\Sigma \leftarrow \Sigma$ bands, and contains only about one percent of the strength of $\Pi \leftarrow \Pi$ bands ($\mathcal{Q} = 1$ as in $21^{13}3-01^{10}$). Equation (3-2) also gives the strengths of lines in the P- and R-branches of $\Pi \leftarrow \Pi$ bands. Gray and Selvidge⁹ have tabulated values of partition functions and relative line strengths for different types of CO_2 bands at several temperatures.

According to quantum theory,¹⁰ the relative strength of the difference band $21^{13}3-01^{10}$ to its associated summation band 20^{03} is given by

$$\begin{aligned} \frac{S_v(21^{13}3-01^{10})}{S_v(20^{03})} &= 2 \exp(-hc 667.4/k\theta) \\ &= 0.078 \text{ for } \theta = 296^\circ\text{K.} \end{aligned} \quad (3-3)$$

h is Planck's constant, c is the speed of light and the factor 2 arises from the double degeneracy of the 01^{10} state. 667.4 cm^{-1} is the difference between the energy levels 01^{10} and 00^{00} .

Equation (3-3) also relates the strength of any difference band to its associated summation or fundamental band if the proper degeneracy factor is used and 667.4 is replaced by the difference between the energy level 00^{00} and the lower level for the difference band.

The strengths of all the bands of significance in the region are given in Table 3-1. From Equations (3-1) and (2-1), we see that the units of band strength are $\text{atm}^{-1} \text{cm}^{-1} \text{cm}^{-1}_{\text{STP}}$, with the STP referring to the absorber thickness and not to the temperature at which the measurement was made.

Since the 20^{03} and $21^{13}3-01^{10}$ bands are not separated in our spectra, their strengths were calculated from their combined strengths by the use of Equation (3-3). The R- and P-branches could be measured separately, and their relative strengths are in good agreement with what we obtain by summing the strengths of the lines in each branch as given by (3-2). The summation gives 52% for the R-branch and 48% for the P-branch.

The R-branch of the 12^{03} band is isolated from other bands and could be measured separately. But the P-branch is overlapped by the $13^{13}3-01^{10}$ band, making it necessary to use Equation (3-3) to determine their strengths.

The 04^{03} band is displaced from its associated difference band ($05^{13}3-01^{10}$) and could be measured directly. There was only a hint of absorption in our original spectra in the region where $05^{13}3-01^{10}$ should appear. Therefore,

its strength could not be measured; it could, of course, be calculated from the strength of the 04^0_3 band.

No values of uncertainty are presented for the strengths of the difference bands since they would depend on the uncertainties of the associated combination bands and on the error in the theoretical relationship given by Equation (3-2). In some cases the uncertainty of an entire band is slightly less than the sum of the two branches since it is not possible to divide the spectrum exactly to determine the contributions of each branch.

The R-branches of the 10^0_3 and 02^0_3 bands of $C^{12}O_2^{16}$ are relatively free of overlapping lines and were measured separately. Strengths of the $11^{13}3-01^{10}$ band and the P-branch of the 10^0_3 band were determined from Equation (3-3) in the same manner as the bands discussed above.

Although a portion of the P-branch of the 02^0_3 band is overlapped by the $03^{13}3-01^{10}$ band, lines P2 to P34 are isolated. By summing the strengths of lines P2 to P34 as given by Equation (3-2), we found that these lines comprise 90.7% of the strength of the entire P-branch. Therefore, the strength of the P-branch was determined from $\int K(\nu)d\nu/.907$ over the region from the band center to a point midway between P34 and P36. Allowance was made for the contribution of the wings of these lines which would occur outside the interval. The correction was calculated by assuming the lines have a Lorentz line shape and a half-width of 1.3 cm^{-1} . (This value of half-width is based on results shown in Section 3.3.) It was not necessary to calculate the correction very accurately since it amounted to only a couple percent of the strength of the P-branch.

The strength of the $03^{13}3-01^{10}$ band was then determined from $\int K(\nu)d\nu$ over the interval covered by the band and subtracting the portion due to the P-branch of the 02^0_3 band. It was also necessary to account for the overlapping 10^0_3 band of $C^{13}O_2^{16}$. By this method we were able to obtain values for the strengths of a combination band and its associated difference band with only a rather small correction based on a theoretical relationship. We see that the relative strengths are $1.0 \times 10^{-4}/11.8 \times 10^{-4} = 0.085$, which agrees, within experimental error, with 0.078 given by Equation (3-3).

The percent of uncertainty for the strength of the 10^0_3 band of $C^{13}O_2^{16}$ is large because of the sizeable corrections which had to be made for the overlapping bands. The strength given for this band is based on samples in which the relative abundances of the various isotopes were not intentionally altered. If we assume that the sample contains 98.9% C^{12} and 1.1% C^{13} , we would expect that, at least in the first approximation, the strengths of the bands of the two isotopes would be in the same ratio. This is seen to be true within experimental error. The ratio of strengths is $2.5 \times 10^{-5}/17.0 \times 10^{-4} = 0.015$, with approximately 40% uncertainty; and the ratio of abundances = 0.011.

3.3 HALF-WIDTHS OF ABSORPTION LINES

The shape of a collision-broadened CO_2 absorption line within a few cm^{-1} of its center, can usually be represented by the Lorentz line shape equation,^{5,11}

$$k(\nu) = \frac{S_m}{\pi} \frac{\alpha}{(\nu - \nu_0)^2 + \alpha^2} \quad (3-4)$$

$k(\nu)$ is the absorption coefficient of the single line; S_m is its strength, ν_0 is the line center, and α is the half-width. α is proportional to pressure while S_m and ν_0 are constant.

Ladenberg and Reiche¹² have shown that the integrated absorptance $\int A(\nu) d\nu$ of a single line having the Lorentz shape is given by

$$\int A(\nu) d\nu = 2\pi\alpha \mathcal{F}(x), \quad (3-5)$$

where $x = Su/2\pi\alpha$, and

$$\mathcal{F}(x) = x e^{-x} \left[J_0(x) - i J_1(x) \right]. \quad (3-6)$$

$J_0(x)$ and $J_1(x)$ are the Bessel functions of order 0 and 1, respectively.

Although Equation (3-6) is a rather involved expression, two well-known approximations can be readily used for single lines under certain conditions:

$$\int A(\nu) d\nu = S_m u, \quad \text{for small } x \quad (\text{weak lines}) \quad (3-7)$$

and

$$\int A(\nu) d\nu = 2 (S_m u \alpha)^{1/2} \quad \text{for large } x \quad (\text{strong lines}). \quad (3-8)$$

It is noted that Equations (3-7) and (3-1) are equivalent for small $A(\nu)$. Values of $\mathcal{F}(x)$ for intermediate x have been tabulated by Kaplan and Eggers.¹³

It is apparent from Equation (3-8) that α can be determined from a measurement of $\int A(\nu) d\nu$ under the proper conditions if S_m is known. $\int A(\nu) d\nu$ is seen to be independent of α for small x and proportional to $\alpha^{1/2}$ for large x . The dependence is less than square root for intermediate x ; and even if the conditions for Equation (3-8) are not fulfilled, α can still be determined by use of the exact expression given by Equation (3-5), provided x is sufficiently large that there is a sizeable dependence on α .

Lines P2 to P32 of the 02^0_3 band are isolated from other lines of any significance; therefore, it was possible to measure $\int A(\nu)d\nu$ for them. Values of S_m were obtained from the band strength given in Table 3-1 by the use of Equation (3-2); and values of $\int A(\nu)d\nu$ were taken from Table 5-2 for each line. The absorber thickness u for Samples 6, 7 and 8 is great enough that x is sufficiently large for a near square-root dependence of $\int A(\nu)d\nu$ on α .

We assumed α^0 (α at a pressure of 1 atm) to be 0.09 cm^{-1} and used Equation (3-5) along with the tabulated values of $\int A(\nu)d\nu$ to calculate $\int A(\nu)d\nu$ for these samples. The calculated values of $\int A(\nu)d\nu$ were then compared with the observed values; and, by a reiterative process, more accurate values of α^0 were obtained.

In making the calculations, we accounted for slight overlapping of the lines which causes the integrated absorbance of a region containing several lines to be less than the sum of the individual contributions we would expect without overlapping. The maximum correction to the calculated $\int A(\nu)d\nu$ for overlapping was only about 5 percent. Results of a recent theoretical article by Plass¹⁴ were used to calculate the overlapping correction factor.

The results of the α^0 measurements are shown by the plotted points in Fig. 3-4; the various geometrical figures correspond to different samples from which the measurement was made. Much of the variation between values for adjacent lines is due to the lines being close together and not completely resolved in the spectra because of the slitwidth of the spectrometer. $\int A(\nu)d\nu$ was calculated between points midway, to the nearest 0.1 cm^{-1} , between line centers. Because of the "rounding-off" of the position of the midpoint and because of slight calibration errors, part of the integral which should be attributed to one line might be attributed to its neighbor.

The solid line represents a mean value of α^0 for lines P6 to P20 in the 00^0_3 band which was determined by us.⁸ The dotted curve was obtained from an empirical equation relating α^0 to J which is given by Winters, Silverman and Benedict.¹¹ The equation is based on data in the 15 μ region by Madden.¹⁵

We see that there is reasonably good agreement among the sets of data for J between about 10 and 22. But beyond $J = 22$, the curve based on Winters, Silverman and Benedict drops off quickly while there is only a hint of drop-off in our data. The uncertainty for an average of our points is probably less than 0.01 cm^{-1} .

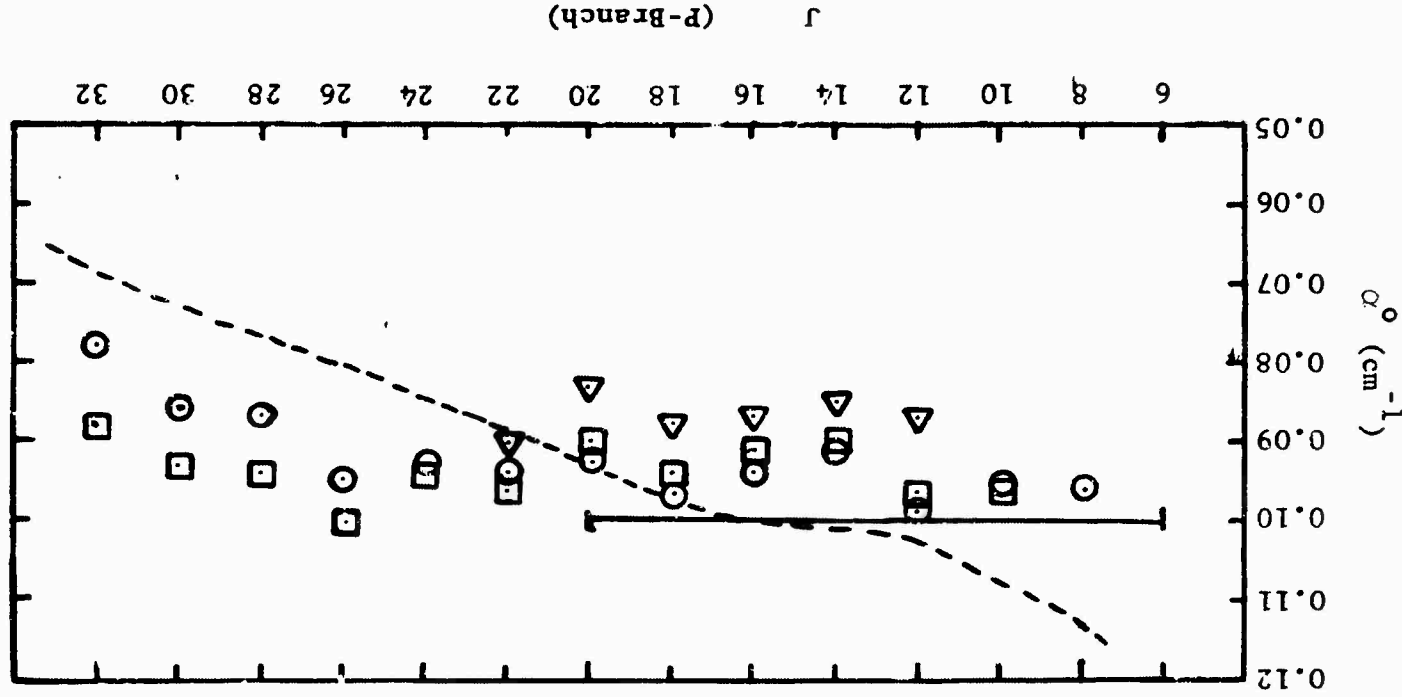


Fig. 3-4. HALF-WIDTHS OF SELF-BROADENED CO₂ LINES
AT 1 ATM PRESSURE

The various geometrical figures correspond to measurements based on different samples: △, 6; ○, 7, and □, 9. Solid curve represents mean value for 003 band. Broken curve represents empirical equation by Winters, Silverman and Benedict¹ based on 010 band.

(This page is intentionally left blank.)

SECTION 4

TABLES OF TRANSMITTANCE

Tables 4-1 and 4-2 consist of values of transmittance, in percent, in the regions 9340 to 9660 cm^{-1} and 8030 to 8340 cm^{-1} , respectively. Values are recorded at intervals of 1 cm^{-1} in Table 4-1 and at intervals of 0.2 cm^{-1} in Table 4-2. In both cases the interval is sufficiently small that the original spectra could be approximated very closely by plotting the tabulated values and joining the points with straight lines. The first and second columns give the wavenumber in vacuum in cm^{-1} and the wavelength in microns.

The sample pressure p and absorber thickness u for each sample are shown at the top of the corresponding column. Each sample is designated by the same number as in Table 3-2 and in the spectra shown in Section 3.

Values are not tabulated over some portions of the spectra of the smaller samples where the absorbance is very small. $T(\nu)$ can be considered as $1 (A(\nu) \approx 0)$, for even the largest samples, from 9415 to 9430 cm^{-1} and from 9530 to 9570 cm^{-1} . Several of the spectra from which the tables were obtained, particularly those between 9340 and 9660 cm^{-1} , represent the average of two or three original spectra which were scanned for the same sample. The wavenumber scale was calibrated by using the known positions of the lines indicated in Figures 3-1 and 3-2.

Table 4-1

[illegible]

Table 4-2

Wavelength (m)	3	4	5	6	7	8	9	10	11	12	13	14
Wavelength (m)	15	16	17	18	19	20	21	22	23	24	25	26
Wavelength (m)	27	28	29	30	31	32	33	34	35	36	37	38
Wavelength (m)	39	40	41	42	43	44	45	46	47	48	49	50
Wavelength (m)	51	52	53	54	55	56	57	58	59	60	61	62
Wavelength (m)	63	64	65	66	67	68	69	70	71	72	73	74
Wavelength (m)	75	76	77	78	79	80	81	82	83	84	85	86
Wavelength (m)	87	88	89	90	91	92	93	94	95	96	97	98
Wavelength (m)	99	100	101	102	103	104	105	106	107	108	109	110
Wavelength (m)	111	112	113	114	115	116	117	118	119	120	121	122
Wavelength (m)	123	124	125	126	127	128	129	130	131	132	133	134
Wavelength (m)	135	136	137	138	139	140	141	142	143	144	145	146
Wavelength (m)	147	148	149	150	151	152	153	154	155	156	157	158
Wavelength (m)	159	160	161	162	163	164	165	166	167	168	169	170
Wavelength (m)	171	172	173	174	175	176	177	178	179	180	181	182
Wavelength (m)	183	184	185	186	187	188	189	190	191	192	193	194
Wavelength (m)	195	196	197	198	199	200	201	202	203	204	205	206
Wavelength (m)	207	208	209	210	211	212	213	214	215	216	217	218
Wavelength (m)	219	220	221	222	223	224	225	226	227	228	229	230
Wavelength (m)	231	232	233	234	235	236	237	238	239	240	241	242
Wavelength (m)	243	244	245	246	247	248	249	250	251	252	253	254
Wavelength (m)	255	256	257	258	259	260	261	262	263	264	265	266
Wavelength (m)	267	268	269	270	271	272	273	274	275	276	277	278
Wavelength (m)	279	280	281	282	283	284	285	286	287	288	289	290
Wavelength (m)	291	292	293	294	295	296	297	298	299	300	301	302
Wavelength (m)	303	304	305	306	307	308	309	310	311	312	313	314
Wavelength (m)	315	316	317	318	319	320	321	322	323	324	325	326
Wavelength (m)	327	328	329	330	331	332	333	334	335	336	337	338
Wavelength (m)	339	340	341	342	343	344	345	346	347	348	349	350
Wavelength (m)	351	352	353	354	355	356	357	358	359	360	361	362
Wavelength (m)	363	364	365	366	367	368	369	370	371	372	373	374
Wavelength (m)	375	376	377	378	379	380	381	382	383	384	385	386
Wavelength (m)	387	388	389	390	391	392	393	394	395	396	397	398
Wavelength (m)	399	400	401	402	403	404	405	406	407	408	409	410
Wavelength (m)	411	412	413	414	415	416	417	418	419	420	421	422
Wavelength (m)	423	424	425	426	427	428	429	430	431	432	433	434
Wavelength (m)	435	436	437	438	439	440	441	442	443	444	445	446
Wavelength (m)	447	448	449	450	451	452	453	454	455	456	457	458
Wavelength (m)	459	460	461	462	463	464	465	466	467	468	469	470
Wavelength (m)	471	472	473	474	475	476	477	478	479	480	481	482
Wavelength (m)	483	484	485	486	487	488	489	490	491	492	493	494
Wavelength (m)	495	496	497	498	499	500	501	502	503	504	505	506
Wavelength (m)	507	508	509	510	511	512	513	514	515	516	517	518
Wavelength (m)	519	520	521	522	523	524	525	526	527	528	529	530
Wavelength (m)	531	532	533	534	535	536	537	538	539	540	541	542
Wavelength (m)	543	544	545	546	547	548	549	550	551	552	553	554
Wavelength (m)	555	556	557	558	559	560	561	562	563	564	565	566
Wavelength (m)	567	568	569	570	571	572	573	574	575	576	577	578
Wavelength (m)	579	580	581	582	583	584	585	586	587	588	589	590
Wavelength (m)	591	592	593	594	595	596	597	598	599	600	601	602
Wavelength (m)	603	604	605	606	607	608	609	610	611	612	613	614
Wavelength (m)	615	616	617	618	619	620	621	622	623	624	625	626
Wavelength (m)	627	628	629	630	631	632	633	634	635	636	637	638
Wavelength (m)	639	640	641	642	643	644	645	646	647	648	649	650
Wavelength (m)	651	652	653	654	655	656	657	658	659	660	661	662
Wavelength (m)	663	664	665	666	667	668	669	670	671	672	673	674
Wavelength (m)	675	676	677	678	679	680	681	682	683	684	685	686
Wavelength (m)	687	688	689	690	691	692	693	694	695	696	697	698
Wavelength (m)	699	700	701	702	703	704	705	706	707	708	709	710
Wavelength (m)	711	712	713	714	715	716	717	718	719	720	721	722
Wavelength (m)	723	724	725	726	727	728	729	730	731	732	733	734
Wavelength (m)	735	736	737	738	739	740	741	742	743	744	745	746
Wavelength (m)	747	748	749	750	751	752	753	754	755	756	757	758
Wavelength (m)	759	760	761	762	763	764	765	766	767	768	769	770
Wavelength (m)	771	772	773	774	775	776	777	778	779	780	781	782
Wavelength (m)	783	784	785	786	787	788	789	790	791	792	793	794
Wavelength (m)	795	796	797	798	799	800	801	802	803	804	805	806
Wavelength (m)	807	808	809	810	811	812	813	814	815	816	817	818
Wavelength (m)	819	820	821	822	823	824	825	826	827	828	829	830
Wavelength (m)	831	832	833	834	835	836	837	838	839	840	841	842
Wavelength (m)	843	844	845	846	847	848	849	850	851	852	853	854
Wavelength (m)	855	856	857	858	859	860	861	862	863	864	865	866
Wavelength (m)	867	868	869	870	871	872	873	874	875	876	877	878
Wavelength (m)	879	880	881	882	883	884	885	886	887	888	889	890
Wavelength (m)	891	892	893	894	895	896	897	898	899	900	901	902
Wavelength (m)	903	904	905	906	907	908	909	910	911	912	913	914
Wavelength (m)	915	916	917	918	919	920	921	922	923	924	925	926
Wavelength (m)	927	928	929	930	931	932	933	934	935	936	937	938
Wavelength (m)	939	940	941	942	943	944	945	946	947	948	949	950
Wavelength (m)	951	952	953	954	955	956	957	958	959	960	961	962
Wavelength (m)	963	964	965	966	967	968	969	970	971	972	973	974
Wavelength (m)	975	976	977	978	979	980	981	982	983	984	985	986
Wavelength (m)	987	988	989	990	991	992	993	994	995	996	997	998
Wavelength (m)	999	1000	1001	1002	1003	1004	1005	1006	1007	1008	1009	1010
Wavelength (m)	1011	1012	1013	1014	1015	1016	1017	1018	1019	1020	1021	1022
Wavelength (m)	1023	1024	1025	1026	1027	1028	1029	1030	1031	1032	1033	1034
Wavelength (m)	1035	1036	1037	1038	1039	1040	1041	1042	1043	1044	1045	1046
Wavelength (m)	1047	1048	1049	1050	1051	1052	1053	1054	1055	1056	1057	1058
Wavelength (m)	1059	1060	1061	1062	1063	1064	1065	1066	1067	1068	1069	1070
Wavelength (m)	1071	1072	1073	1074	1075	1076	1077	1078	1079	1080	1081	1082
Wavelength (m)	1083	1084	1085	1086	1087	1088	1089	1090	1091	1092	1093	1094
Wavelength (m)	1095	1096	1097	1098	1099	1100	1101	1102	1103	1104	1105	1106
Wavelength (m)	1107	1108	1109	1110	1111	1112	1113	1114	1115	1116	1117	1118
Wavelength (m)	1119	1120	1121	1122	1123	1124	1125	1126	1127	1128	1129	1130
Wavelength (m)	1131	1132	1133	1134	1135	1136	1137	1138	1139	1140	1141	1142
Wavelength (m)	1143	1144	1145	1146	1147	1148	1149	1150	1151	1152	1153	1154
Wavelength (m)	1155	1156	1157	1158	1159	1160	1161	1162	1163	1164	1165	1166
Wavelength (m)	1167	1168	1169	1170	1171	1172	1173	1174	1175	1176	1177	1178
Wavelength (m)	1179	1180	1181	1182	1183	1184	1185	1186	1187	1188	1189	1190
Wavelength (m)	1191	1192	1193	1194	1195	1196	1197	1198	1199	1200	1201	1202
Wavelength (m)	1203	1204	1205	1206	1207	1208	1209	1210	1211	1212	1213	1214
Wavelength (m)	1215	1216	1217	1218	1219	1220	1221	1222	1223	1224	1225	1226
Wavelength (m)	1227	1228	1229	1230	1231	1232	1233	1234	1235	1236	1237	1238
Wavelength (m)	1239	1240	1241	1242	1243	1244	1245	1246	1247	1248	1249	1250
Wavelength (m)	1251	1252	1253	1254	1255	1256	1257	1258	1259	1260	1261	1262
Wavelength (m)	1263	1264	1265	1266	1267	1268	1269	1270	1271	1272	1273	1274
Wavelength (m)	1275	1276	1277	1278	1279	1280	1281	1282	1283	1284	1285	1286
Wavelength (m)	1287	1288	1289	1290	1291	1292	1293	1294	1295	1296	1297	1298
Wavelength (m)	1299	1300	1301	1302	1303	1304	1305	1306	1307	1308	1309	1310
Wavelength (m)	13											

Table 4-2 (continued)

[illegible]

Table 4-2 (continued)

[illegible]

Table 4-2 (continued)

Year, Dec	1	2	3	4	5	6	7	8	9	10	11	12	13	14	15	16	17	18	19	20	21	22	23	24	25	26	27	28	29	30	31	32	33	34	35	36	37	38	39	40	41	42	43	44	45	46	47	48	49	50	51	52	53	54	55	56	57	58	59	60	61	62	63	64	65	66	67	68	69	70	71	72	73	74	75	76	77	78	79	80	81	82	83	84	85	86	87	88	89	90	91	92	93	94	95	96	97	98	99	100																																																																																																																																																																																					
1950	1.22240	1.22241	1.22242	1.22243	1.22244	1.22245	1.22246	1.22247	1.22248	1.22249	1.22250	1.22251	1.22252	1.22253	1.22254	1.22255	1.22256	1.22257	1.22258	1.22259	1.22260	1.22261	1.22262	1.22263	1.22264	1.22265	1.22266	1.22267	1.22268	1.22269	1.22270	1.22271	1.22272	1.22273	1.22274	1.22275	1.22276	1.22277	1.22278	1.22279	1.22280	1.22281	1.22282	1.22283	1.22284	1.22285	1.22286	1.22287	1.22288	1.22289	1.22290	1.22291	1.22292	1.22293	1.22294	1.22295	1.22296	1.22297	1.22298	1.22299	1.22300	1.22301	1.22302	1.22303	1.22304	1.22305	1.22306	1.22307	1.22308	1.22309	1.22310	1.22311	1.22312	1.22313	1.22314	1.22315	1.22316	1.22317	1.22318	1.22319	1.22320	1.22321	1.22322	1.22323	1.22324	1.22325	1.22326	1.22327	1.22328	1.22329	1.22330	1.22331	1.22332	1.22333	1.22334	1.22335	1.22336	1.22337	1.22338	1.22339	1.22340	1.22341	1.22342	1.22343	1.22344	1.22345	1.22346	1.22347	1.22348	1.22349	1.22350	1.22351	1.22352	1.22353	1.22354	1.22355	1.22356	1.22357	1.22358	1.22359	1.22360	1.22361	1.22362	1.22363	1.22364	1.22365	1.22366	1.22367	1.22368	1.22369	1.22370	1.22371	1.22372	1.22373	1.22374	1.22375	1.22376	1.22377	1.22378	1.22379	1.22380	1.22381	1.22382	1.22383	1.22384	1.22385	1.22386	1.22387	1.22388	1.22389	1.22390	1.22391	1.22392	1.22393	1.22394	1.22395	1.22396	1.22397	1.22398	1.22399	1.22400	1.22401	1.22402	1.22403	1.22404	1.22405	1.22406	1.22407	1.22408	1.22409	1.22410	1.22411	1.22412	1.22413	1.22414	1.22415	1.22416	1.22417	1.22418	1.22419	1.22420	1.22421	1.22422	1.22423	1.22424	1.22425	1.22426	1.22427	1.22428	1.22429	1.22430	1.22431	1.22432	1.22433	1.22434	1.22435	1.22436	1.22437	1.22438	1.22439	1.22440	1.22441	1.22442	1.22443	1.22444	1.22445	1.22446	1.22447	1.22448	1.22449	1.22450	1.22451	1.22452	1.22453	1.22454	1.22455	1.22456	1.22457	1.22458	1.22459	1.22460	1.22461	1.22462	1.22463	1.22464	1.22465	1.22466	1.22467	1.22468	1.22469	1.22470	1.22471	1.22472	1.22473	1.22474	1.22475	1.22476	1.22477	1.22478	1.22479	1.22480	1.22481	1.22482	1.22483	1.22484	1.22485	1.22486	1.22487	1.22488	1.22489	1.22490	1.22491	1.22492	1.22493	1.22494	1.22495	1.22496	1.22497	1.22498	1.22499	1.22500	1.22501	1.22502	1.22503	1.22504	1.22505	1.22506	1.22507	1.22508	1.22509	1.22510	1.22511	1.22512	1.22513	1.22514	1.22515	1.22516	1.22517	1.22518	1.22519	

Table 4-2 (continued)

[illegible]

Table 4-2 (continued)

Table 4-2 (continued)

Year, Mo.	1	2	3	4	5	6	7	8	9	10	11	12	13	14
Day	1	2	3	4	5	6	7	8	9	10	11	12	13	14
Time	1	2	3	4	5	6	7	8	9	10	11	12	13	14
Temp.	1	2	3	4	5	6	7	8	9	10	11	12	13	14
Wind	1	2	3	4	5	6	7	8	9	10	11	12	13	14
Pressure	1	2	3	4	5	6	7	8	9	10	11	12	13	14
Humidity	1	2	3	4	5	6	7	8	9	10	11	12	13	14
Clouds	1	2	3	4	5	6	7	8	9	10	11	12	13	14
Visibility	1	2	3	4	5	6	7	8	9	10	11	12	13	14
Wind Dir.	1	2	3	4	5	6	7	8	9	10	11	12	13	14
Wind Spd.	1	2	3	4	5	6	7	8	9	10	11	12	13	14
Wave Hgt.	1	2	3	4	5	6	7	8	9	10	11	12	13	14
Water Level	1	2	3	4	5	6	7	8	9	10	11	12	13	14
Ice	1	2	3	4	5	6	7	8	9	10	11	12	13	14
Remarks	1	2	3	4	5	6	7	8	9	10	11	12	13	14
9820.0	1.20144	1.20145	1.20146	1.20147	1.20148	1.20149	1.20150	1.20151	1.20152	1.20153	1.20154	1.20155	1.20156	1.20157
9820.1	1.20158	1.20159	1.20160	1.20161	1.20162	1.20163	1.20164	1.20165	1.20166	1.20167	1.20168	1.20169	1.20170	1.20171
9820.2	1.20172	1.20173	1.20174	1.20175	1.20176	1.20177	1.20178	1.20179	1.20180	1.20181	1.20182	1.20183	1.20184	1.20185
9820.3	1.20186	1.20187	1.20188	1.20189	1.20190	1.20191	1.20192	1.20193	1.20194	1.20195	1.20196	1.20197	1.20198	1.20199
9820.4	1.20200	1.20201	1.20202	1.20203	1.20204	1.20205	1.20206	1.20207	1.20208	1.20209	1.20210	1.20211	1.20212	1.20213
9820.5	1.20214	1.20215	1.20216	1.20217	1.20218	1.20219	1.20220	1.20221	1.20222	1.20223	1.20224	1.20225	1.20226	1.20227
9820.6	1.20228	1.20229	1.20230	1.20231	1.20232	1.20233	1.20234	1.20235	1.20236	1.20237	1.20238	1.20239	1.20240	1.20241
9820.7	1.20242	1.20243	1.20244	1.20245	1.20246	1.20247	1.20248	1.20249	1.20250	1.20251	1.20252	1.20253	1.20254	1.20255
9820.8	1.20256	1.20257	1.20258	1.20259	1.20260	1.20261	1.20262	1.20263	1.20264	1.20265	1.20266	1.20267	1.20268	1.20269
9820.9	1.20270	1.20271	1.20272	1.20273	1.20274	1.20275	1.20276	1.20277	1.20278	1.20279	1.20280	1.20281	1.20282	1.20283
9821.0	1.20284	1.20285	1.20286	1.20287	1.20288	1.20289	1.20290	1.20291	1.20292	1.20293	1.20294	1.20295	1.20296	1.20297
9821.1	1.20298	1.20299	1.20300	1.20301	1.20302	1.20303	1.20304							

Table 4-2 (continued)

[illegible]

SECTION 5

TABLES OF INTEGRATED ABSORPTANCE

Values of the integrated absorptance are presented in Tables 5-1 and 5-2 for the 9430-9660 cm^{-1} and 8030-8340 cm^{-1} intervals, respectively. The integrals were calculated from the transmittance tables in Section 4 by assuming that the spectrum could be constructed by plotting the transmittance values and joining them with straight lines.

The lower limit of integration ν' , which is shown at the top of each column, was chosen at a point where there was essentially no absorption. The integrated absorptance between any two wavenumbers listed can be found by subtracting the values tabulated at those two points. Values are tabulated at intervals of 5 cm^{-1} in Table 5-1 which covers samples whose spectra have but little structure. Table 5-2 includes samples whose spectra have considerable structure. Throughout most of the region, the integral is tabulated at points midway between the absorption lines. In regions where the spectra are smooth, tabulations are made at intervals of 5 or 10 cm^{-1} .

Table 5-1 $\left[\int_v^{\infty} A(v) dv \right]$

Sam. No.	P (atm)	U (atm cm)	V (cm ³)
4	2.50 2.17 2.10 2.05	1.63 2.17 1.63 1.63	V = .9370 V = .9370 V = .9370 V = .9370
3	2.50 2.17 2.10 2.05	1.63 2.17 1.63 1.63	V = .9370 V = .9370 V = .9370 V = .9370
2	2.50 2.17 2.10 2.05	1.63 2.17 1.63 1.63	V = .9370 V = .9370 V = .9370 V = .9370
1	2.50 2.17 2.10 2.05	1.63 2.17 1.63 1.63	V = .9370 V = .9370 V = .9370 V = .9370

Table 5-2 $\left[\int_{\nu} \dot{A}(\nu) d\nu \right]$ [illegible]

(This page is left intentionally blank.)

SECTION 6

REFERENCES

1. G. Herzberg and L. Herzberg, J. Opt. Soc. Am. 43, 1037 (1953).
2. D. E. Burch, D. A. Gryvnak and R. R. Patty, Absorption of CO₂ Between 4500 and 5400 cm⁻¹, Aeronutronic Report U-2955, Contract NOnr 3560(00), (15 December 1964).
3. D. E. Burch, R. R. Patty and D. A. Gryvnak, Absorption and Emission of Infrared Radiation by CO₂ and H₂O, Aeronutronic Report U-2367, Contract NOnr 3560(00), (26 November 1963).
4. D. E. Burch, D. A. Gryvnak and Dudley Williams, Appl. Opt. 1, 759, (1962).
5. D. E. Burch, D. A. Gryvnak, R. R. Patty and Charlotte Bartky, The Shapes of Collision-Broadened CO₂ Absorption Lines, Aeronutronic Report U-3203, Contract NOnr 3560(00), (1965).
6. C. P. Courtoy, Annales de la Societe Scientifique de Bruxelles, Serie 1, pp 5-230 (27 March 1959). Also, C. P. Courtoy, Canad. J. Phys. 35, 608 (1957).
7. V. R. Stull, P. J. Wyatt and G. N. Plass, The Infrared Absorption of Carbon Dioxide, Aeronutronic Report U-1505, Contract AF 19(604)-7479, (30 December 1961).
8. D. E. Burch, D. A. Gryvnak and R. R. Patty, Absorption by CO₂ Between 6600 and 7125 cm⁻¹ (1.4 Micron Region), Aeronutronic Report U-3127, Contract NOnr 3560(00), (1965).
9. L. D. Gray and J. E. Selvidge, J. Quant. Spectros. Radiat. Transfer 5, 291, (1965).
10. G. Herzberg, Infrared and Raman Spectra of Polyatomic Molecules, D. Van Nostrand Co. (See 266 ff for a discussion of the intensities of difference bands) (Ninth printing 1960).

REFERENCES

(Continued)

11. B. H. Winters, S. Silverman and W. S. Benedict, J. Quant. Spec. 4, 527 (1964).
12. R. Ladenberg and F. Reiche, Ann. Physik 42, 181 (1913).
13. L. D. Kaplan and D. F. Eggers, Jr., J. Chem. Phys. 25, 876 (1956).
14. G. N. Plass, J. Opt. Soc. Am. 55, 104 (1965).
15. R. P. Madden, J. Chem. Phys 35, No. 6, 2083 (1961).